5-17-2006

Image fusion for improved perception

Michel Ouendeno

Samuel Peter Kozaitis

Image fusion for improved perception

M. Ouendeno and S. P. Kozaitis
Florida Institute of Technology
Department of Electrical and Computer Engineering
150 W. University Blvd.
Melbourne, FL 32901

ABSTRACT

We developed a method to fuse imagery for from different sensor types. The core of our method uses different forward transforms of input images and a common transform to reconstruct the final result. When measuring the entropy and power of the fused result, we found that our method gave generally better results when compared to a more conventional approach. Our method could form the basis of a new image fusion approach because it offers results not possible with a conventional approach.

Keywords: image fusion, image transform, wavelet, wavelet transform

1. INTRODUCTION

There are several methods commonly employed today to combine imagery from different sensors during image fusion processing.[1-3] In many cases, such as with cross-sensor imagery, a compromised solution occurs due to non-optimal retention of information from each source. Typically, the fused solution favors one set of information characteristics over the other in a non-optimal manner. The more straightforward methods use a linear combination of images, such as pixel averaging, some sort of pixel-by-pixel comparison by energy, or a projection method, such as principle component analysis (PCA). Usually the focus has been on the fusion rule, or how to combine imagery. The common thread between current fusion methods is that regardless of how they combine images, they are fundamentally limited by their reconstruction treatments. When data from different sensors are used, one of two cases exists. The reconstruction must favor one type of sensor over the other causing a loss in information in one set of data. Or, the reconstruction favors neither sensor (an average for example), and the reconstruction is not optimal for either sensor resulting a loss in information content in the fused product.

We developed a new method for combining cross-sensor image data that preserves sensor-unique characteristics of each contributing sensor while optimizing the extraction of information from the resultant fused product. The basis of our approach is a set of forward wavelet transforms, optimized to preserve the individual information content of each sensor image followed by a common inverse transform that is designed to simultaneously preserve the most desirable information characteristics from each image after fusion. Using the method proposed here, we expect to reconstruct a fused image that will retain the information content from disparate domains while enhancing the information content of the fused image product. Our has broad applicability to any image fusion problem involving sensor data having different spatial, spectral or temporal characteristics. We envision a broad applications space for this approach in tactical processing environments where layered surveillance architectures result in a rich set of diverse image products that must be quickly and optimally combined.

2. FUSION

Data fusion can be thought of combining two signals represented as vectors $\mathbf{x}_1$ and $\mathbf{x}_2$ and somehow extracting the maximum amount of information. Often, transform methods are used because the

Signal Processing, Sensor Fusion, and Target Recognition XV, edited by Ivan Kadar,
Proc. of SPIE Vol. 6235, 62351D, (2006) · 0277-786X/06/$15 · doi: 10.1117/12.666476

signals can be represented more compactly in the transform domain, than in the time or spatial domain. In matrix form, the transforms of $\mathbf{x}_1$ and $\mathbf{x}_2$ are $\mathbf{A}\mathbf{x}_1$ and $\mathbf{A}\mathbf{x}_2$ respectively, where $\mathbf{A}$ is a matrix and represents a transform. Combining the signals in the transform domain is represented as

$$\mathbf{g} = f(\mathbf{A}\mathbf{x}_1, \mathbf{A}\mathbf{x}_2), \tag{1}$$

where $f(\ )$ represents a fusion function or rule. Then, the resultant image is obtained through the inverse transform as $\mathbf{r} = \mathbf{A}^{-1}\mathbf{g}$, where the signal $\mathbf{r}$ represents the fusion of the two signals in the spatial domain. However, if the input signals are from disparate sensors, then finding a transform $\mathbf{A}$, that say, maximizes $\|\mathbf{g}\|$ for $\mathbf{x}_1$, may not do so for $\mathbf{x}_2$. If an $\mathbf{A}$ is found that works similarly for both signals, then the value of $\|\mathbf{g}\|$ may not be maximized.

In our approach, we attempted to use different forward transforms, $\mathbf{A}_1$, $\mathbf{A}_2$ for signals from disparate sensors. If such an approach is successful, it could offer many new solutions to data fusion problems because we can use many combinations of transforms rather than just one. The fused image, $\mathbf{g}$ can be represented as

$$\mathbf{g} = f(\mathbf{A}_1\mathbf{x}_1, \mathbf{A}_2\mathbf{x}_2), \tag{2}$$

the combination of images in the wavelet domain due to some rule f. Because $\mathbf{A}_1$ and $\mathbf{A}_2$ are often square matricies, if their inverses exists; they are unique. Therefore, the transforms operating on the two input signals must be the same if the reconstruction error,

$$e = \| \, |\mathbf{R}\mathbf{A}_1| + |\mathbf{R}\mathbf{A}_2| - 2\mathbf{I} \, \|, \tag{3}$$

is zero, where $\mathbf{R}$ represents the inverse transform. However, if the input signals are from disparate sensors, then finding an inverse transform $\mathbf{R}$, that say, maximizes $\|\mathbf{g}\|$ and minimizes the portion of e due to $\mathbf{A}_1$, may not minimize the portion of e due to $\mathbf{A}_2$, and vice versa.

Our goal is to choose $\mathbf{A}_1$, $\mathbf{A}_2$, and $\mathbf{R}$ to maximize $\|\mathbf{g}\|$ while optimizing some metric. In this way, we expect to transfer the maximum amount of information to the fused image $\mathbf{r}$. Our solution to the fusion problem uses the wavelet transforms. Wavelet transforms offer a convenient framework for image reconstruction in this case, and therefore is well-suited to signal fusion. The wavelet transform typically compacts energy efficiently, and may use a variety of basis functions. The wavelet transform can be represented as a matrix as

$$\mathbf{W} = \begin{bmatrix} \mathbf{L} \\ \mathbf{B} \end{bmatrix} \tag{4}$$

where $\mathbf{W}$ is equivalent to $\mathbf{A}_1$, or $\mathbf{A}_2$, and the submatrices $\mathbf{L}$ and $\mathbf{B}$ represent the dual bases of the wavelet transform, the scaling and wavelet functions respectively. We considered different transforms for the two input signals, and for the synthesis (inverse) transform so that,

$$\mathbf{A}_1 = \begin{bmatrix} \mathbf{L}_1 \\ \mathbf{B}_1 \end{bmatrix},\ \mathbf{A}_2 = \begin{bmatrix} \mathbf{L}_2 \\ \mathbf{B}_2 \end{bmatrix}, \text{ and } \mathbf{R} = \begin{bmatrix} \mathbf{L}_3 & \mathbf{B}_3 \end{bmatrix}. \tag{5}$$

Wavelet and scaling functions are usually complicated to describe, and implementation often employs digital filter banks. Therefore, wavelet and scaling functions are usually specified through filter coefficients. The wavelet transform can be efficiently implemented in terms of filter banks consisting of filters and decimators. Usually, a two-channel filter bank is used with low-pass and high-pass filters. The low-pass, and high-pass filters of the forward transform are, $LF(z)$ and $HF(z)$, and the low-pass, and high-pass filters of the inverse transform are, $LI(z)$ and $HI(z)$. A block diagram of two filter banks indicating the two forward transforms, where each is equivalent to one level of a wavelet transform is shown Fig. 1, where the subscripts indicate whether the filters belong to $\mathbf{A}_1$ or $\mathbf{A}_2$. The goal of our work is to choose an appropriate $LI_1(z) = LI_2(z)$ and $HI_1(z) = HI_2(z)$.

If we consider only one level of the transform, then the **L**'s and **B**'s in Eq. 5 can be viewed as low- and high-pass filters, and written in the z-domain as,

$$\begin{array}{lll} \mathbf{L}_1 \rightarrow LF_1(z), & \mathbf{L}_2 \rightarrow LF_2(z), & \mathbf{L}_3 \rightarrow LI_3(z) = LI_1(z) = LI_2(z), \\ \mathbf{B}_1 \rightarrow HF_1(z), & \mathbf{B}_2 \rightarrow HF_2(z), & \mathbf{B}_3 \rightarrow HI_3(z) = LI_1(z) = LI_2(z). \end{array} \tag{6}$$

We wanted the wavelets in the forward transforms to be different so they could have different characteristics to better represent signals from disparate sensors. Therefore, we allowed $HF_1(z) \neq HF_2(z)$, and set $LF_1(z) = LF_2(z)$ to relate the two transforms.

In wavelet transforms, the high-pass filter of the synthesis transform is related to the low-pass filter of the forward transform. Therefore we set the high-pass filter of **R** to

$$HF_3(z) = -LF_1(-z) = -LF_2(-z). \tag{7}$$

If we choose $HF_1(z)$ and $HF_2(z)$ based on the characteristics of the sensors and the type of features we are considering, then the problem reduces to finding a suitable $LI_3(z)$. A block diagram of the system is shown in Fig. 2.

3. EXPERIMENT

In our experiments we considered different biorthogonal transforms for $\mathbf{A}_1$, $\mathbf{A}_2$, and **R,** with different filters for each transform. The fusion rule was one where the maximum value of the wavelet coefficients was used on a pixel-by-pixel basis between the two image transform results. For the lower subbands of the image not processed by a wavelet, we used a linear combination between the transforms.

Since the fusion rule transfers the maximum amount of energy to the result, we examined the amount of energy in the result for various situations. We also considered the entropy of the fused image as defined as

$$H = -\sum_{i=1}^{G} d(i)\log_2\{di)\}, \tag{8}$$

where G is the number of gray levels in the image, and $d(i)$ is the normalized histogram.[4] The entropy is used here to generally measure the change in information between input images and the fused result. We used the set of 512 x 512 images as shown in Figs. 3 and 4 in our experiments and used three levels of the wavelet transform. The entropy of the input images and their mutual information for the images in Fig. 3 is shown in Table 1.

Table 1 Results of fusion experiments for images in Fig. 3

Wavelet Filters											
A1	A2	A3	Entropy		Mutual Info	Entropy of Fused Images			Energy of Fused images		
			Input 1	Input 2		C1	C2	C3	C1	C2	C3
1.1	1.5	1.3	5.615	6.806	0.683	**6.137**	6.061	6.121	**3.51**	3.50	**3.51**
1.5	1.3	1.1	5.615	6.806	0.683	6.092	**6.292**	6.244	3.50	**3.54**	3.53
1.3	1.1	1.5	5.615	6.806	0.683	6.094	**6.112**	6.091	3.50	**3.51**	3.50
2.2	2.6	2.4	5.615	6.806	0.683	**6.154**	6.113	6.126	**3.51**	**3.51**	**3.51**
2.6	2.4	2.2	5.615	6.806	0.683	6.220	**6.399**	6.351	3.52	**3.56**	3.55
2.4	2.2	2.6	5.615	6.806	0.683	6.114	6.130	**6.143**	**3.51**	**3.51**	**3.51**
3.5	3.3	3.1	5.615	6.806	0.683	6.195	**7.181**	7.119	3.52	**3.91**	3.86

We considered the entropy of the fused result for three different cases, C1, C2, and C3. The case C1 corresponds to where both forward transforms, and the inverse transform equal $\mathbf{A}_1$. This is the conventional case for image fusion. The case C2 corresponded to, one forward transform equal to $\mathbf{A}_2$, the other equal to $\mathbf{A}_3$, and the inverse equal to $\mathbf{A}_1$. Finally, case C3 corresponded to one forward transform equal to $\mathbf{A}_2$, the other equal to $\mathbf{A}_3$, and the inverse equal to $\mathbf{A}_2$. In this case, the inverse transform favors one of the images. The wavelets used were from the Wavelet Toolbox in the commercial package Matlab. The values of entropy of the fused results were usually between that of the two images, but in one case the fused entropy was higher. In most cases the entropy was greatest in case C2. In addition, in all cases the energy in the fused result was greatest with C2 even through the energy was similar to other cases for some wavelets.

Similar results were found for the images in Fig. 4. However, the fusion results had higher values of entropy than the input images, and the case C2 always had the greatest entropy. In addition, the energy in fused image was usually largest in the case of C2. For both sets of images, sample results for the case of C2 with the largest entropy are shown in Fig. 5.

Table 2 Results of fusion experiments for images in Fig 4

Wavelet Filters											
A1	A2	A3	Entropy		Mutual Info	Entropy of Fused Images			Energy of Fused images		
			Imag1	Imag2		C1	C2	C3	C1	C2	C3
2.6	2.4	2.2	7.213	7.136	0.9244	7.556	**7.672**	7.623	2.77	**2.85**	2.82
2.4	2.2	2.6	7.213	7.136	0.9244	7.557	**7.626**	7.598	2.77	**2.81**	2.78
3.1	3.5	3.3	7.213	7.136	0.9244	8.050	**8.606**	7.650	3.35	**4.82**	2.83
3.5	3.3	3.1	7.213	7.136	0.9244	7.581	**8.386**	8.281	2.78	**4.14**	3.85
3.3	3.1	3.5	7.213	7.136	0.9244	7.618	**8.248**	8.242	2.81	3.60	**3.75**

4 CONCLUSION

We developed a method to fuse imagery from different sensors. The core of our method uses different forward transforms of images and a common transform for reconstruction. Using the wavelet transform, we were able to use different high-pass filters for the forward transform. In this way, the transforms can be tailored to specific type of imagery such as infrared and visible. We used the same low-pass filters in the forward transforms to relate the two transforms, and derived the synthesis high-pass filter from this filter. When measuring the entropy, and the energy of the fused result, we found that our method gave generally better results when compared to a more conventional approach. A better metric should be investigated because entropy could be increased when the noise is increased. Our method could form the basis of a new image fusion approach because it offers results not possible with a conventional approach.

REFERENCES

1. D. A. Socolinsky, and L. B. Wolff, "Multi-spectral image visualization through first order fusion," *IEEE Transactions on Image Processing*, 11, 923-931, 2002.

2. P. Scheunders, "An orthogonal wavelet representation of multivalued images," *IEEE Transactions on Image Processing*, 12(6), 718-725, 2003.

3. V. S. Petrovic, and C. S. Xydeas, "Gradient-based Multiresolution Image Fusion," *IEEE Transactions on Image Processing*, 13(2), 228-237, 2004.

4. L. W. Leung, B. King, and V. Vohora, "Comparison of image data fusion techniques using entropy and INI", *22nd Asian Conference on Remote Sensing*, Nov. 5-9, 2001, Singapore.

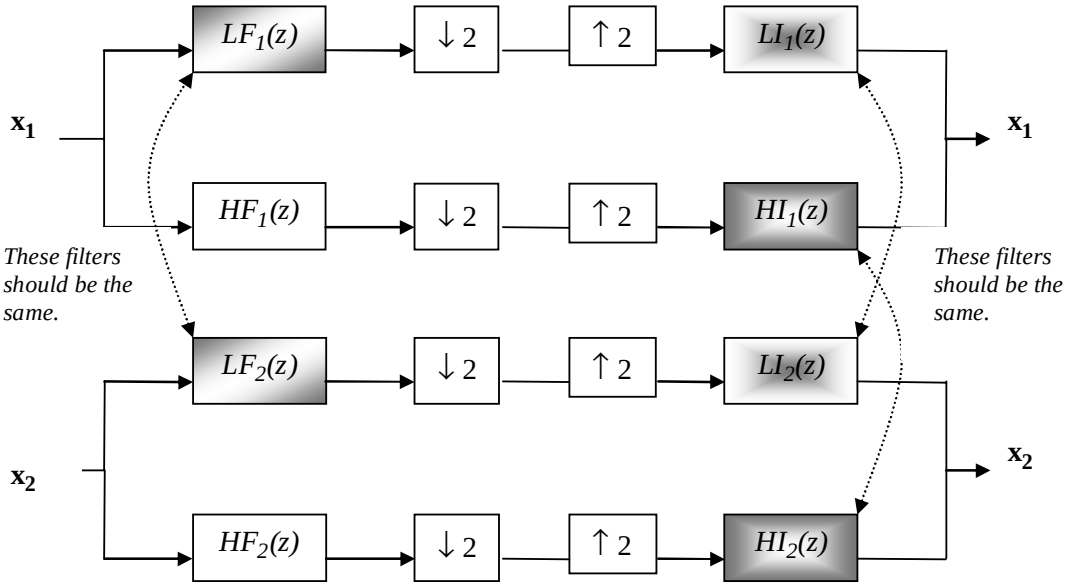

Figure 1 Two filter banks and their inverses each representing one level of the wavelet transform.

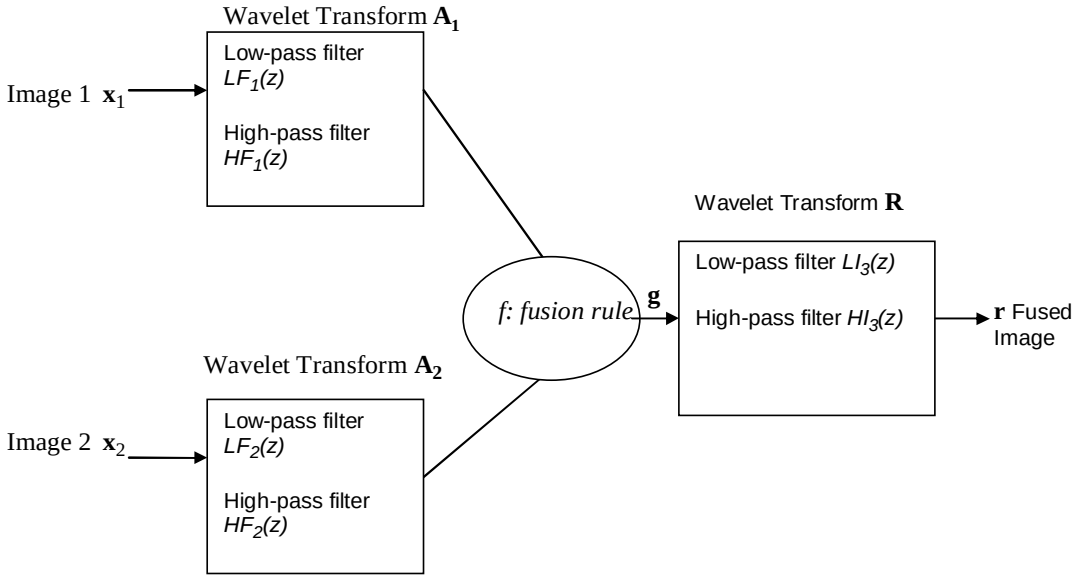

Figure 2 Block diagram of image fusion process.

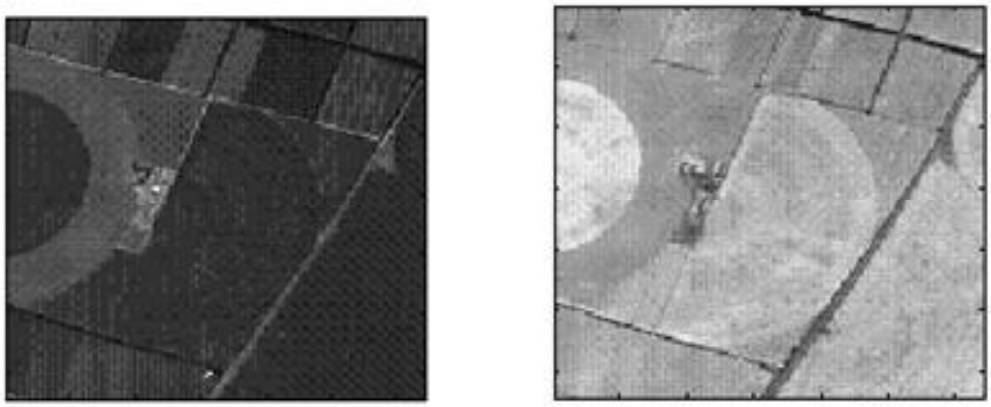

Figure 3 Input images used in experiments.

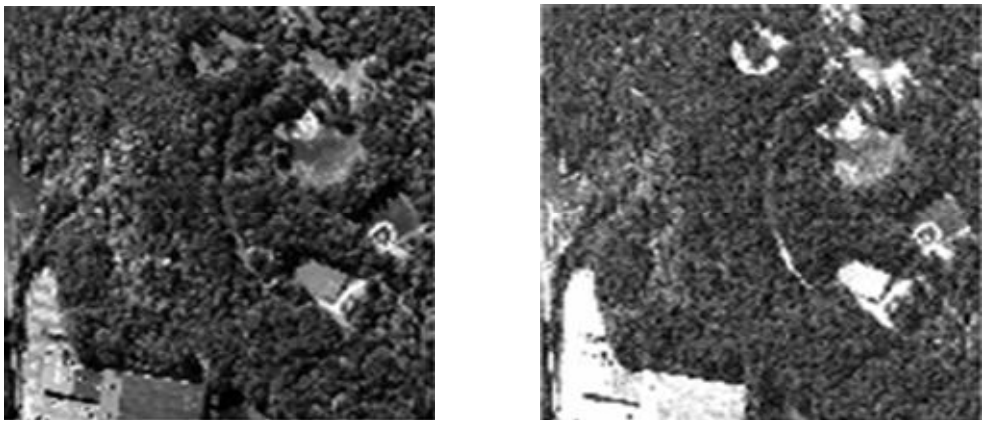

Figure 4 Input images used in experiments.

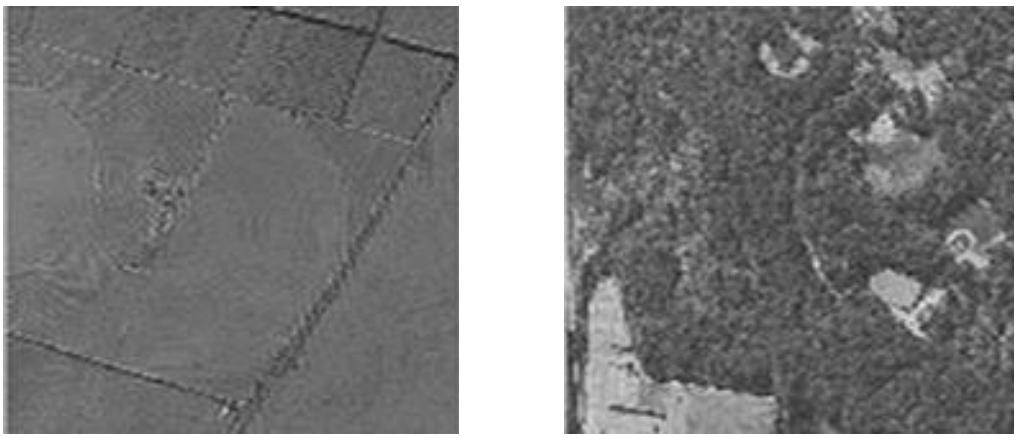

(a) (b)

Figure 5 Image fusion results (a) from images in Fig. 3 (b) from images in Fig. 4.